

Exploring the nature of the fergusonite–scheelite phase transition and ionic conductivity enhancement by Mo⁶⁺ doping in LaNbO₄

Josie E. Auckett, Laura Lopez-Odriozola, Stewart J. Clark and Ivana R. Evans

Supporting Information

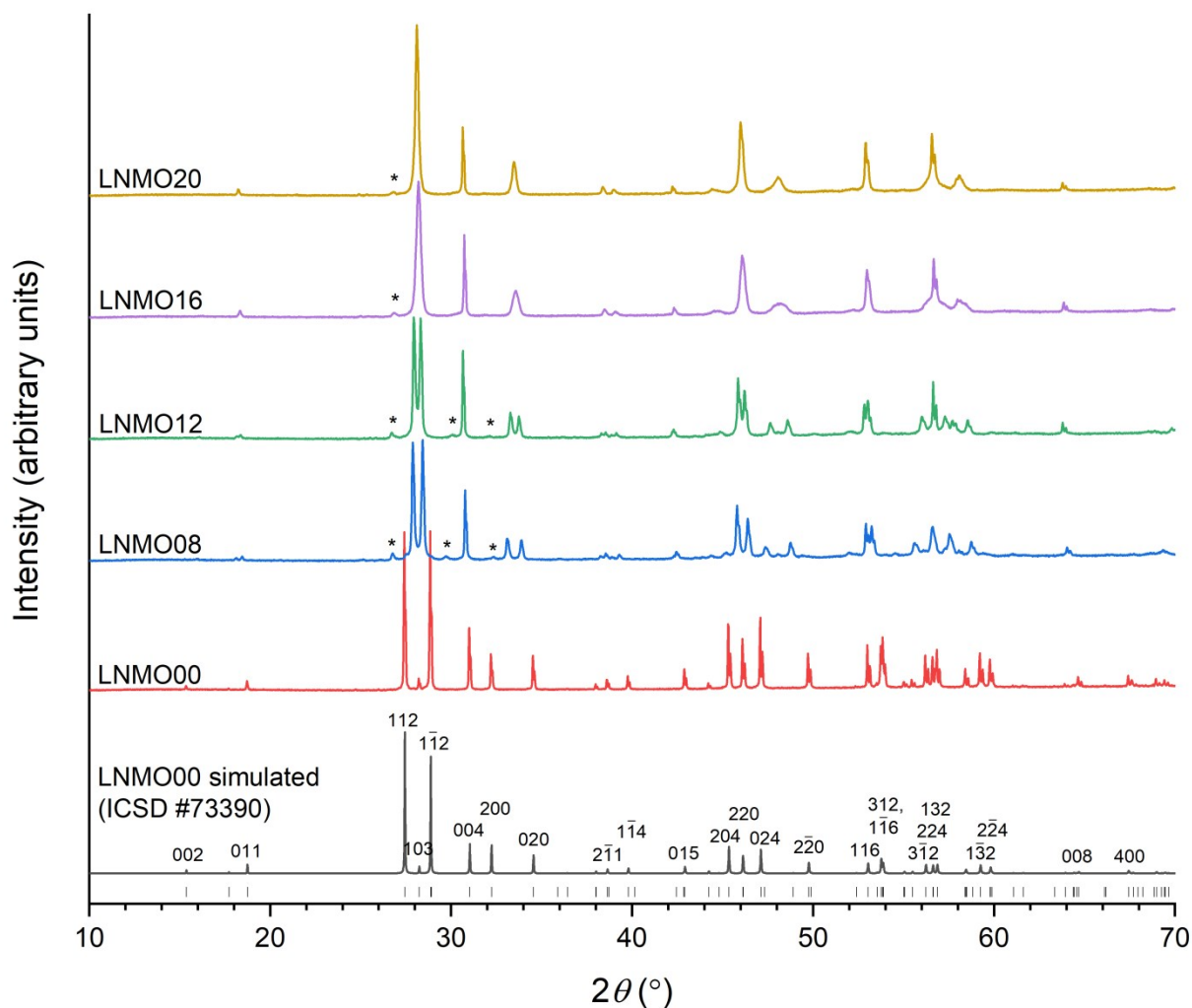


Figure S1. Powder x-ray diffraction profiles of as-made samples of LaNb_{1-x}Mo_xO_{4+0.5x} (LNMO). Indices marked above the simulated pattern correspond to a unit cell obtained by transforming the ICSD reference structure into a setting with *I*2/*b* symmetry (*c* > *a* > *b*; *γ* < 90°) for better comparability with the tetragonal scheelite structure. Asterisks denote reflections that are considered to arise from structure modulations, by analogy to LaNb_{1-x}W_xO_{4+0.5x}.¹

Sample	Range division (°C)	α_V , low T range ($\times 10^{-6} \text{ K}^{-1}$)	α_V , high T range ($\times 10^{-6} \text{ K}^{-1}$)
LNMO00	500	16.4	9.3
LNMO08	600	11.8	11.7
LNMO12	650	11.9	15.5
LNMO16	600	11.0	14.1
LNMO20	450	10.4	13.4

Table S1. Average linear thermal expansion coefficients derived from linear fitting to the refined lattice volumes (manuscript Figure 1(d)) above and below a range division point chosen arbitrarily to maximise the goodness of fit in each region.

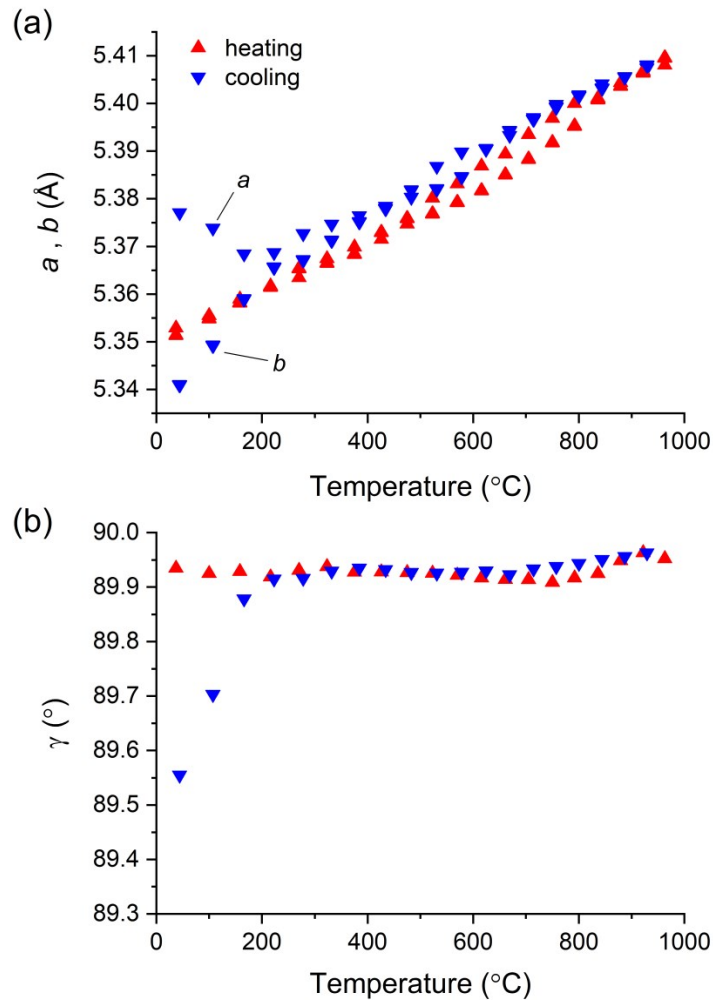


Figure S2. Comparison of lattice parameters of LNMO20 refined against VT-XRD data recorded upon heating and cooling. Error bars are smaller than the symbols.

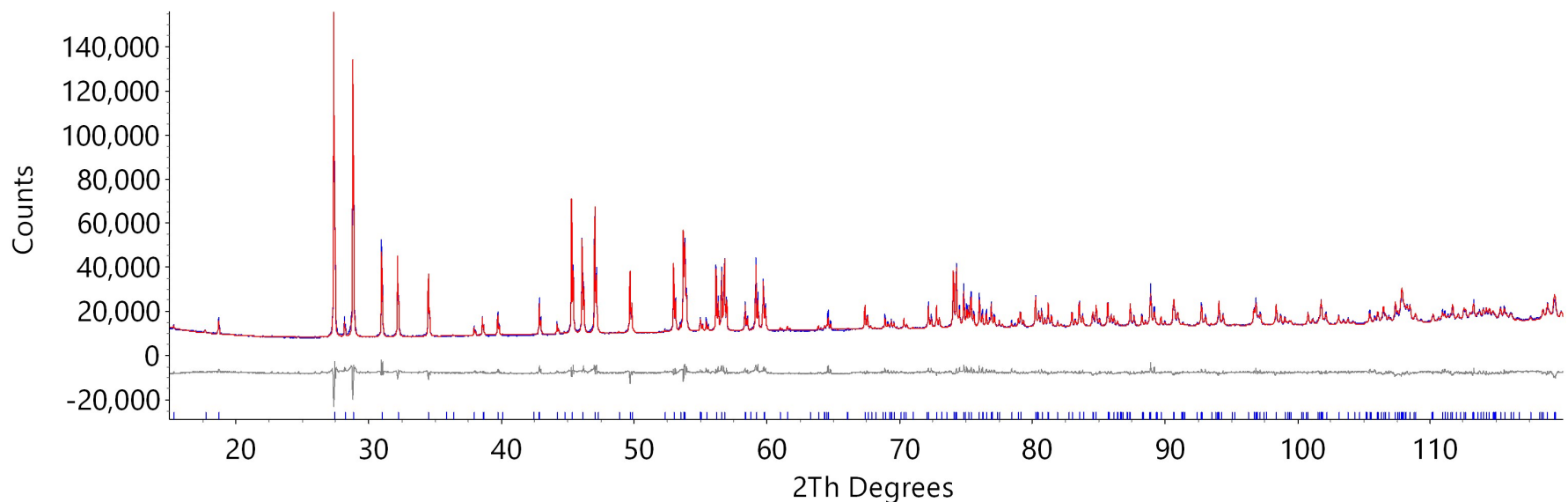


Figure S3. Laboratory x-ray diffraction data (Cu K α radiation) recorded for LaNbO₄ at room temperature (blue line), and the fit obtained by symmetry distortion mode Rietveld refinement (red line) while refining the amplitudes of eight symmetry-adapted distortion modes. (Grey line: difference between observed and calculated plots; blue markers: positions of Bragg reflections. $R_{wp} = 3.66\%$, $R_{Bragg} = 2.80\%$)

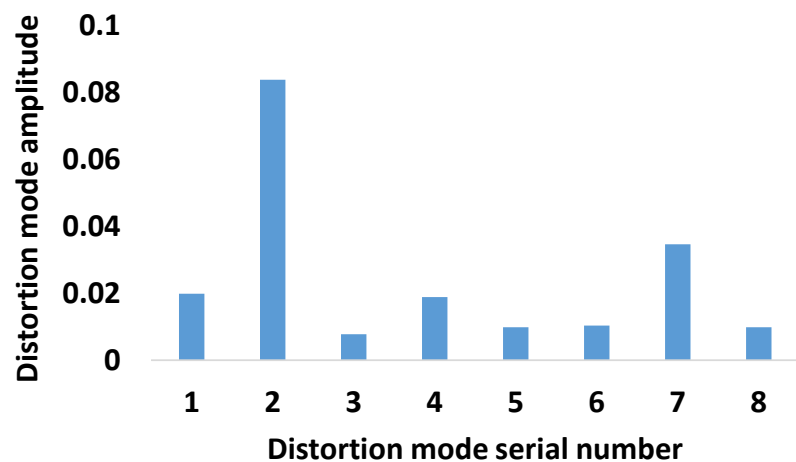


Figure S4. Amplitudes of the eight distortion modes refined in the distortion mode analysis depicted in Figure S3.

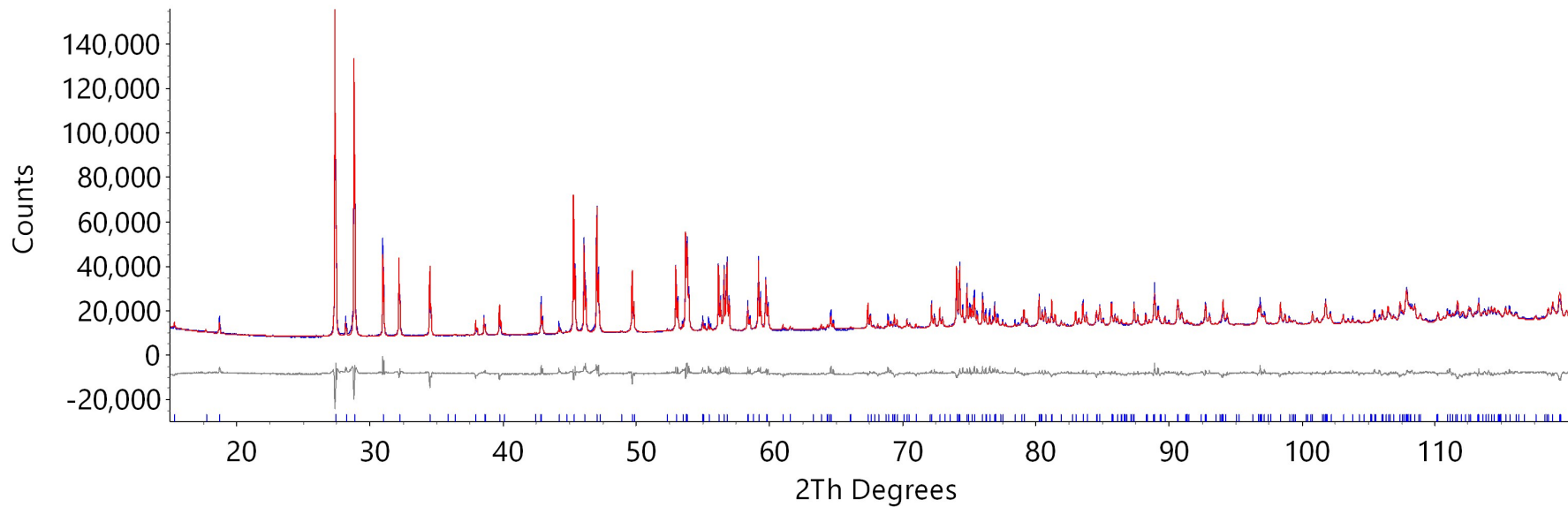


Figure S5. Symmetry distortion mode Rietveld refinement fit to the same data shown in Figure S3, while refining only the amplitude of the most significant symmetry-adapted distortion mode (a2) out of eight possible modes. (Blue line: observed; red line: calculated; grey line: difference between observed and calculated; blue markers: positions of Bragg reflections. $R_{wp} = 4.20\%$, $R_{Bragg} = 3.28\%$)

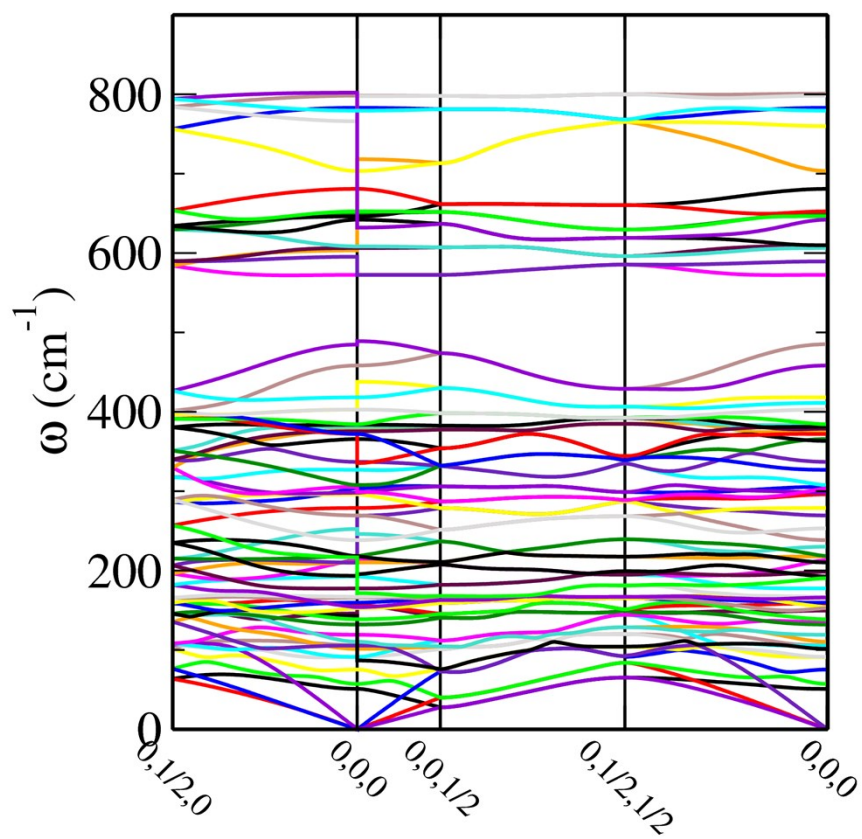


Figure S6. Phonon dispersion curves calculated for fergusonite-type LaNbO_4 at 37°C .

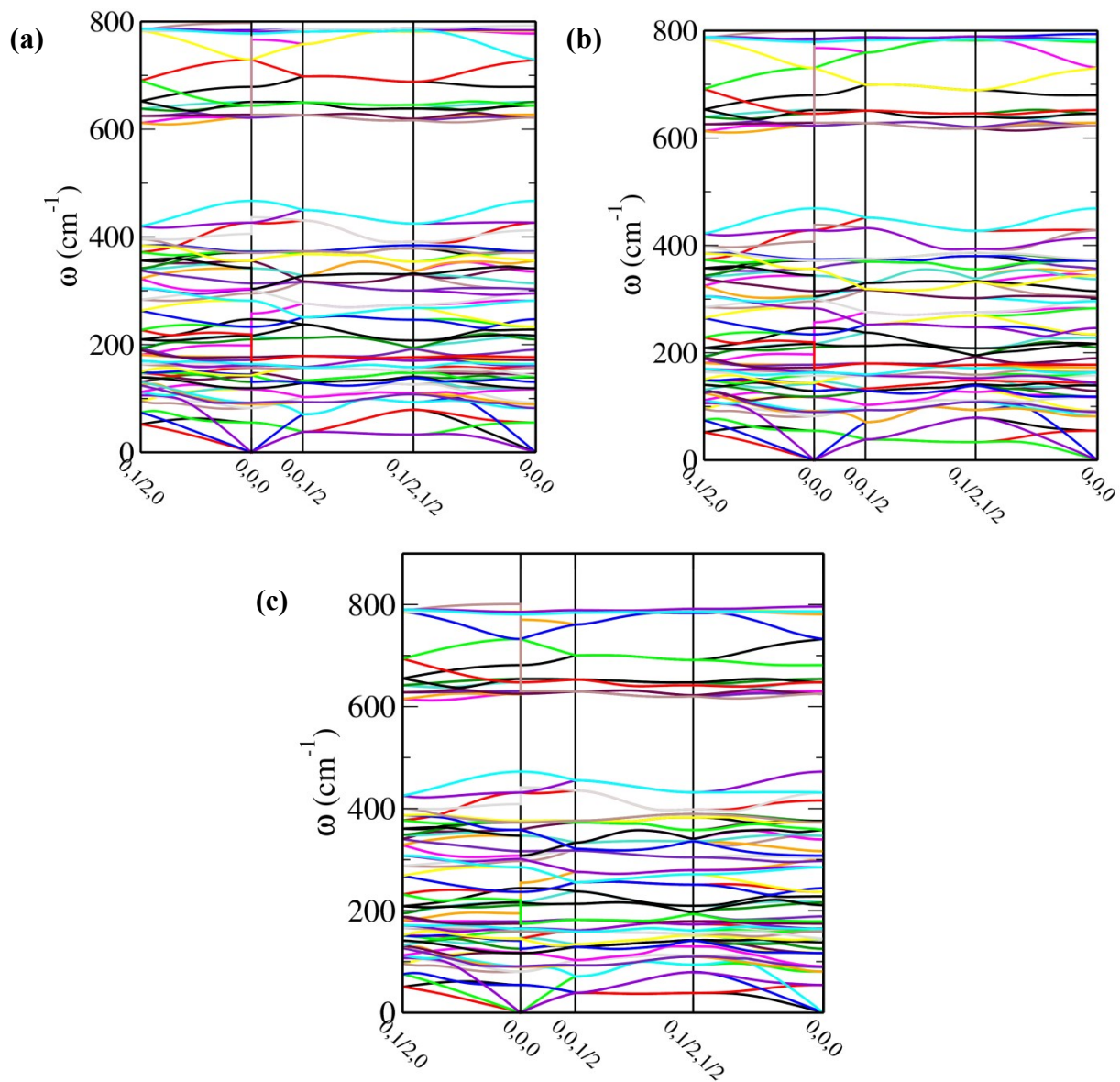


Figure S7. Phonon dispersion curves calculated for scheelite-type LaNbO_4 at (a) 477 °C, (b) 377 °C and (c) 177 °C. Line colours are assigned independently for each plot and do not necessarily represent corresponding phonon modes in different plots.

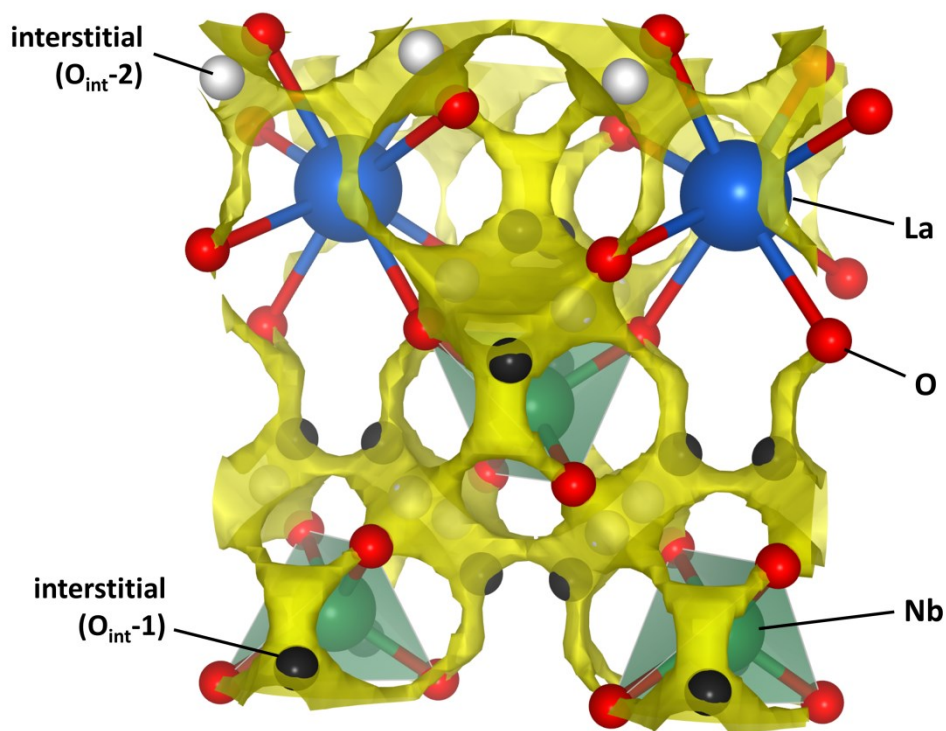


Figure S8. Section of a bond valence energy landscape (BVEL) map calculated for a DFT-optimised $2 \times 2 \times 1$ supercell of undoped LaNbO₄ using 3DBVSMAPPER.² Black and white atoms mark the positions of O²⁻ interstitial sites denoted by Toyoura *et al.*³ as O_{int-1} and O_{int-2}, respectively (these sites are drawn for indication only and were not included in the BVEL calculation). The BVEL map is drawn at an isolevel of +0.90 eV above the minimum energy value in the interconnected pathway. (Figure prepared using VESTA⁴)

LNMO16					
Observation	Nb	Mo	La	Mo/(Mo+Nb)	(Mo+Nb)/total
Centre #1	10.86	2.19	13.19	0.168	0.497
Centre #2	11.19	2.19	13.61	0.164	0.496
Centre #3	11.19	2.21	13.71	0.165	0.494
Centre #4	10.72	2.20	12.84	0.170	0.502
Centre #5	10.77	2.03	12.90	0.159	0.498
Centre #6	10.81	1.98	13.36	0.155	0.489
Average				0.163	0.496
Standard Dev.				0.005	0.004
Edge #1	12.26	2.43	14.59	0.165	0.502
Edge #2	11.12	2.23	13.70	0.167	0.494
Edge #3	12.19	2.38	14.88	0.163	0.495
Edge #4	11.53	2.44	14.17	0.175	0.496
Average				0.168	0.497
Standard Dev.				0.004	0.003
Expected value				0.16	0.50
LNMO20					
Observation	Nb	Mo	La	Mo/(Mo+Nb)	(Mo+Nb)/total
Centre #1	11.54	2.93	15.21	0.202	0.488
Centre #2	11.94	2.98	15.52	0.200	0.490
Centre #3	12.03	3.15	15.54	0.208	0.494
Centre #4	11.57	2.86	15.23	0.198	0.487
Average				0.202	0.490
Standard Dev.				0.004	0.003
Edge #1	12.12	3.06	14.99	0.202	0.503
Edge #2	12.02	2.81	15.45	0.189	0.490
Edge #3	11.75	2.78	15.03	0.191	0.492
Edge #4	11.88	3.03	15.05	0.203	0.498
Average				0.196	0.496
Standard Dev.				0.005	0.006
Expected value				0.20	0.50

Table S2. Non-normalised relative cation abundances obtained from EDX spectra collected at various points on the surfaces of sintered pellets of LNMO16 and LNMO20. For each sample, measurement points were chosen at random and divided arbitrarily into “Centre” and “Edge” subsets based on their proximity to the pellet edge.

References

- 1 C. Li, R. D. Bayliss and S. J. Skinner, *Solid State Ionics*, 2014, **262**, 530-535.
- 2 M. Sale and M. Avdeev, *J. Appl. Crystallogr.*, 2012, **45**, 1054-1056.
- 3 K. Toyoura, Y. Sakakibara, T. Yokoi, A. Nakamura and K. Matsunaga, *J. Mater. Chem. A*, 2018, **6**, 12004-12011.
- 4 K. Momma and F. Izuma, *J. Appl. Crystallogr.*, 2008, **41**, 653-658.